

Unsaturated binuclear homoleptic metal carbonyls $M_2(CO)_x$ ($M = Fe, Co, Ni$; $x = 5, 6, 7, 8$). Are multiple bonds between transition metals possible for these molecules?*

Henry F. Schaefer III[†] and R. Bruce King

*Department of Chemistry and Center for Computational Quantum Chemistry,
University of Georgia, Athens, Georgia 30602*

Abstract: Modern density functional methods, which yield geometrical parameters and energies close to experimental values for known metal carbonyls such as $Fe(CO)_5$ and $Fe_2(CO)_9$, have been extended to unsaturated binary binuclear metal carbonyls. Novel optimized structures have been discovered containing metal–metal multiple bonds, four-electron bridging carbonyl groups, and metal electronic configurations less than 18 electrons.

INTRODUCTION

Metal carbonyl chemistry originated in 1890 with the serendipitous discovery by Mond, Langer, and Quincke [1] of $Ni(CO)_4$ from the reaction of finely divided nickel with carbon monoxide at atmospheric pressure. This seminal discovery was shortly followed in 1891 by the simultaneous discovery of $Fe(CO)_5$ by Berthelot [2] and by Mond and Quincke [3]. An early study of the chemistry of $Fe(CO)_5$ led to the discovery of the first binuclear metal carbonyl, namely $Fe_2(CO)_9$, formed from the exposure of $Fe(CO)_5$ to light [4]. Subsequent work by Mond, Hirtz, and Cowap [5] led to the discovery of $Co_2(CO)_8$ obtained from the direct combination of finely divided metallic cobalt and carbon monoxide at elevated temperatures. The dimeric nature of $Co_2(CO)_8$ was already established by cryoscopy in benzene in the 1910 paper [5]. In the 90 years since the original report of $Co_2(CO)_8$ no other binuclear binary metal carbonyl of iron, cobalt, or nickel has been isolated in the pure state under normal laboratory conditions, although a few such binuclear metal carbonyls have been identified spectroscopically in low-temperature matrices.

Table 1 summarizes the stoichiometries for possible binuclear binary metal carbonyls of iron, cobalt, and nickel, the three metals of interest in this work. The indicated metal–metal bond order assumes the favored 18-electron rare gas configuration. The “saturated” metal carbonyls in Table 1, namely the known $Fe_2(CO)_9$ and $Co_2(CO)_8$ and the unknown $Ni_2(CO)_7$, may be regarded as metal carbonyl analogs of ethane. Unsaturated binuclear metal carbonyls containing formal metal–metal double, triple, and even quadruple bonds (Table 1) may be regarded analogously as metal carbonyl analogs of ethylene and acetylene. No such unsaturated binuclear metal carbonyls have yet been isolated under normal laboratory conditions although some such species (e.g., $Fe_2(CO)_8$ and $Co_2(CO)_7$) have been identified spectroscopically in low-temperature matrices. However, a variety of unsaturated cyclopentadienylmetal carbonyls containing formal metal–metal double and triple bonds have been prepared and characterized structurally [6]. The first such compound was the molybdenum dimer $(Me_5C_5)_2Mo_2(CO)_4$, originally reported in 1967 by King and Bisnette [7]. This derivative as well as the closely related $(C_5H_5)_2Mo_2(CO)_4$ [8] were subsequently shown by X-ray diffraction [9] to have abnor-

*Lecture presented at the 38th IUPAC Congress/World Chemistry Congress 2001, Brisbane, Australia, 1–6 July 2001. Other presentations are published in this issue, pp. 1033–1145.

[†]Corresponding author

mally short molybdenum–molybdenum distances suggesting the Mo≡Mo triple bond required for the favored 18-electron configuration around each molybdenum atom.

Unsaturated binuclear metal carbonyls can, in principle, be divided into three general structural types:

- (1) Structures containing formal metal–metal multiple bonds with the favored 18-electron rare gas metal electronic configuration. This is the common structural type for unsaturated binuclear cyclopentadienylmetal carbonyls [6].
- (2) Structures containing four-electron bridging carbonyl groups and with a lower metal–metal bond order than otherwise required to accommodate the unsaturation. Such four-electron bridging carbonyl groups, which bond to the metal atom not only through metal–carbon bonds but also through π -donation from the carbon–oxygen multiple bond, are not known in *binuclear* unsaturated cyclopentadienylmetal carbonyls but are found in binuclear manganese compounds of the type (diphos)₂Mn₂(CO)₄(η^2 - μ -CO) (diphos = small bite chelating ditertiary phosphine of the type R₂PCH₂PR₂) first prepared by Colton and Commons in 1975 [10] and characterized structurally shortly thereafter [11].
- (3) Structures in which one or both of the metal atoms have less than the favored 18-electron configuration. Such is probably the case with CoRh(CO)₇, isoelectronic with Co₂(CO)₇ (Table 1), which has been isolated as a thermally unstable yellow solid from the reaction of NaCo(CO)₄ with [Rh(CO)₂Cl]₂ under a CO atmosphere [12]. The instability of CoRh(CO)₇ (decomposition at –65 °C under nitrogen) has so far prevented a structural determination by X-ray diffraction. However, the pattern of infrared ν (CO) frequencies has been interpreted as suggesting a structure with a Co–Rh single bond and a square planar rhodium atom with a 16-electron configuration similar to that in many *d*⁸ square planar Rh(I) complexes [12].

Table 1 Homoleptic binuclear metal carbonyls M₂(CO)_x (M = Fe, Co, Ni), which have been studied computationally in this work (molecules which have been synthesized in the laboratory are indicated in boxes).

	Fe	Co	Ni
M–M	Fe₂(CO)₉	Co₂(CO)₈	Ni ₂ (CO) ₇
M=M	Fe ₂ (CO) ₈	Co ₂ (CO) ₇	Ni ₂ (CO) ₆
M≡M	Fe ₂ (CO) ₇	Co ₂ (CO) ₆	Ni ₂ (CO) ₅
M≡M	Fe ₂ (CO) ₆	Co ₂ (CO) ₅	

The fact that no isolable unsaturated binary binuclear metal carbonyls of the first-row transition-metals were synthesized under normal laboratory conditions in the first 110 years of metal carbonyl chemistry (1890–2000) suggests that such compounds are not synthetically accessible. Thus, attempted thermal or photochemical decarbonylation of the known saturated Fe₂(CO)₉ and Co₂(CO)₈ (Table 1) to give unsaturated binuclear metal carbonyl derivatives under standard laboratory conditions, as opposed to low-temperature matrices, leads instead to the isolation of metal carbonyls of higher nuclearity, namely Fe₃(CO)₁₂ and Co₄(CO)₁₂, respectively, which were the first metal carbonyls to be discovered of higher nuclearity than two [5]. Therefore, computational methods become particularly useful in order to study the chemistry of binary binuclear metal carbonyls including unsaturated derivatives. Calculations on binary metal carbonyls using modern density functional methods are readily performed on modern computers. In cases where experimental data are available for comparison [e.g., Fe(CO)₅ and Fe₂(CO)₉ in Table 2], such methods give computed values for bond distances, bond angles, and vibrational frequencies close to those found experimentally [13]. This provides considerable credibility as to

Table 2 Test of computational methods with Fe(CO)₅ and Fe₂(CO)₉, where experimental data are available for comparison.

For Fe(CO) ₅	DZP BP86	DZP B3LYP	Experimental
Fe–C (ax), Å	1.8053	1.8226	1.811, 1.807
Fe–C (eq), Å	1.8053	1.8158	1.803, 1.827
C–O (ax), Å	1.1673	1.1524	1.117, 1.152
C–O (eq), Å	1.1701	1.1563	1.133, 1.152
For Fe ₂ (CO) ₉	DZP BP86	DZP B3LYP	Experimental
Fe–Fe, Å	2.5188	2.5233	2.523
Fe–C(t), Å	1.8186	1.8288	1.838
Fe–C(b), Å	2.0066	2.0076	2.016
C–O(t), Å	1.1664	1.1516	1.156
C–O(b), Å	1.1862	1.1756	1.176
∠C–Fe–C(t)	95.9°	96.4°	96.1°
∠Fe–C–O(t)	176.9°	177.5°	177.1°

the relevance of such computed information on currently unknown metal carbonyl derivatives to possible future experimental work.

Recently, we initiated computational studies on binuclear metal carbonyl derivatives and related compounds at the University of Georgia. This account presents the highlights of our results for the binary binuclear metal carbonyls of nickel, cobalt, and iron. Further details on these results are presented elsewhere [14–16].

COMPUTATIONAL METHODS

Our basis set for C and O begins with Dunning's standard double- ζ contraction [17] of Huzinaga's primitive sets [18] and is designated (9s5p/4s2p). The double- ζ plus polarization (DZP) basis set used here adds one set of pure spherical harmonic d functions with orbital exponents $\alpha_d(\text{C}) = 0.75$ and $\alpha_d(\text{O}) = 0.85$ to the DZ basis set. For the transition-metals, in our loosely contracted DZP basis set, the Wachters' primitive set [19] is used, but augmented by two sets of p functions and one set of d functions, contracted following Hood *et al.* [20] and designated (14s11p6d/10s8p3d).

Electron correlation effects were included employing density functional theory (DFT) methods, which have been widely proclaimed as a practical and effective computational tool, especially for organometallic compounds. Among density functional procedures, the most reliable approximation is often thought to be the hybrid HF/DFT method using the combination of the three-parameter Becke exchange functional with the Lee–Yang–Parr nonlocal correlation functional known as B3LYP [21,22]. However, another DFT method, which combines Becke's 1988 exchange functional with Perdew's 1986 nonlocal correlation functional method (BP86), was also used in the present paper for comparison [23,24].

We fully optimized the geometries of all structures with both the DZP B3LYP and DZP BP86 methods. At the same levels we have also calculated the vibrational frequencies by evaluating analytically the second derivatives of energy with respect to the nuclear coordinates. The corresponding infrared intensities have been evaluated analytically as well. All of the computations were carried out with the Gaussian 94 program [25] in which the fine grid (75 radial shells, 32 angular points) is the default for evaluating integrals numerically, and the tight (10^{-8} hartree) designation is the default for the SCF convergence.

RESULTS AND DISCUSSION

Nickel carbonyls

No binary nickel carbonyls other than $\text{Ni}(\text{CO})_4$ have been synthesized. The computed optimized structures of the binary binuclear nickel carbonyls (Fig. 1) are all derived from the tetrahedral structure of $\text{Ni}(\text{CO})_4$ by sharing of vertices, edges, and faces to give $\text{Ni}_2(\text{CO})_7$ formulated with a Ni–Ni single bond, $\text{Ni}_2(\text{CO})_6$ formulated with an Ni=Ni double bond, and $\text{Ni}_2(\text{CO})_5$ formulated with an Ni≡Ni triple bond, respectively, in order to conform to the 18-electron rule for each nickel atom. The optimized nickel–nickel distances decrease in the sequence $\text{Ni}_2(\text{CO})_7 > \text{Ni}_2(\text{CO})_6 > \text{Ni}_2(\text{CO})_5$ (Fig. 1) in accord with the increase in the formal nickel–nickel bond order.

Attempts to synthesize these $\text{Ni}_2(\text{CO})_x$ species or other nickel carbonyls with a lower CO/Ni ratio, such as the $\text{Ni}_2(\text{CO})_n$ species discussed in this paper, by thermolysis or photolysis of $\text{Ni}(\text{CO})_4$ have never succeeded. Thus, the only observed anaerobic decomposition product of $\text{Ni}(\text{CO})_4$ has been nickel metal. This contrasts with the corresponding chemistry of $\text{Fe}(\text{CO})_5$, where photolysis of $\text{Fe}(\text{CO})_5$ readily results in loss of 10% of the carbonyl ligands to give $\text{Fe}_2(\text{CO})_9$ by the reaction [26]:



Isolation of $\text{Fe}_2(\text{CO})_9$ from this reaction mixture is facilitated by its insolubility, which means that it can precipitate as it is formed so that it is protected from further reaction. This is actually rather

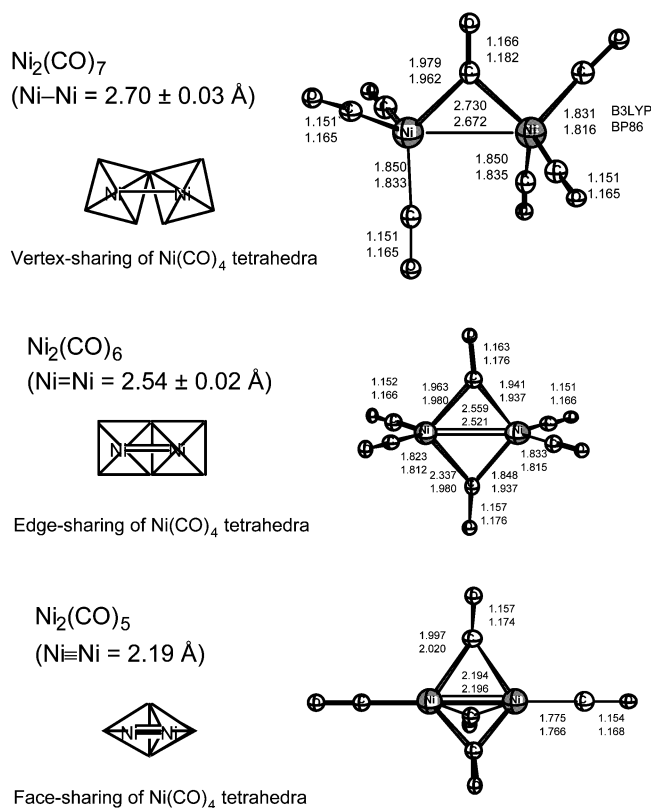


Fig. 1 Computed optimized structures for $\text{Ni}_2(\text{CO})_x$ ($x = 7, 6, 5$) showing their formation by the vertex-, edge-, and face-sharing of $\text{Ni}(\text{CO})_4$ tetrahedra.

important since $\text{Fe}_2(\text{CO})_9$ decomposes only slightly above room temperature to regenerate $\text{Fe}(\text{CO})_5$, as well as a coordinately unsaturated $\text{Fe}(\text{CO})_4$ fragment by the reaction



In the absence of a substrate to trap the $\text{Fe}(\text{CO})_4$ fragment such as a Lewis base ligand to form an $\text{LFe}(\text{CO})_4$ complex [27], the $\text{Fe}(\text{CO})_4$ will trimerize to $\text{Fe}_3(\text{CO})_{12}$, which is the first procedure that was used to prepare this trinuclear carbonyl.

The decomposition temperature of $\text{Fe}(\text{CO})_5$ under a given set of anaerobic reaction conditions appears to be about 100 °C higher than that of $\text{Ni}(\text{CO})_4$. Extrapolation of this ~100 °C decomposition temperature difference from the mononuclear metal carbonyls $\text{M}(\text{CO})_n$ ($\text{M} = \text{Fe}, \text{Ni}$) to the corresponding binuclear metal carbonyls $\text{M}_2(\text{CO})_m$ predicts a decomposition temperature well below room temperature (possibly around -60 °C) for at least $\text{Ni}_2(\text{CO})_7$ if not the other binuclear nickel carbonyls. The comparison of nickel and iron carbonyl chemistry suggests that the best chance for synthesizing any of the binuclear nickel carbonyls would be a low-temperature photolysis (e.g., at -100 °C) of $\text{Ni}(\text{CO})_4$ in a suitable inert solvent. However, use of low-temperature experimental techniques would be essential for isolating $\text{Ni}_2(\text{CO})_y$ without decomposition. This predicted very low decomposition temperature of binary binuclear nickel carbonyls probably accounts for the fact that they have never been isolated.

Despite this pessimism about the prospects of isolating and handling any binary binuclear nickel carbonyls under ambient laboratory conditions, experimental work during the last 30 years has demonstrated the ability to stabilize binuclear nickel carbonyl units by the replacement of four carbonyl groups in μ -carbonylhexacarbonyldinickel [$\text{Ni}_2(\text{CO})_7$] with small bite bidentate ditertiary phosphine ligands to give $(\text{diphos})_2\text{Ni}_2(\text{CO})_2(\mu\text{-CO})$ derivatives [28–30]. Some binuclear nickel carbonyls of this type, which have been isolated and structurally characterized are depicted in Fig. 2. In general, the Ni–Ni bond distances in the structurally characterized $(\text{diphos})_2\text{Ni}_2(\text{CO})_2(\mu\text{-CO})$ derivatives fall in the rather wide range 2.53–2.69 Å, which in general is lower than the 2.73 Å Ni–Ni bond distance calculated for the parent μ -carbonylhexacarbonyldinickel. The stabilization of $\text{Ni}_2(\text{CO})_7$ by such phosphine substitution of carbonyl ligands is typical in metal carbonyl chemistry and arises from an increase in the electron density on the nickel atoms by replacement of CO groups with the weaker π -acceptor phosphine ligands. The apparent shortening of the Ni–Ni single bond distance calculated for $\text{Ni}_2(\text{CO})_7$ by replacement of CO groups with phosphine ligands may also be a consequence of strengthening the Ni–Ni bond through this resulting increase in the metal electron density.

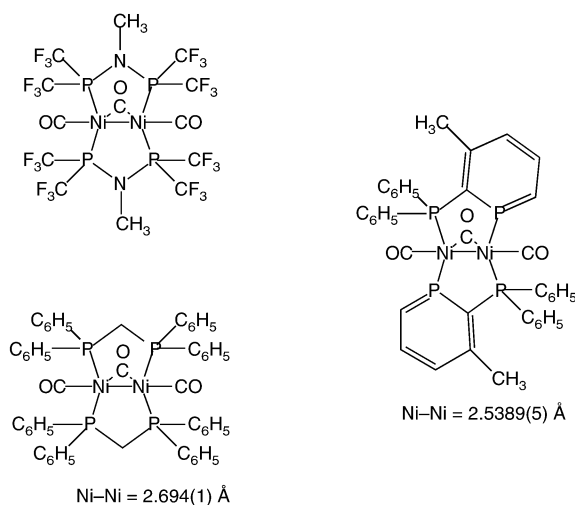


Fig. 2 Some known examples of $(\text{diphos})_2\text{Ni}_2(\text{CO})_2(\mu\text{-CO})$ derivatives.

Cobalt carbonyls

The only binary binuclear cobalt carbonyl synthesized in macroscopic quantities is $\text{Co}_2(\text{CO})_8$, which has been isolated as a C_{2v} dibridged structure (Fig. 3) and characterized structurally [31–33]. However, infrared $\nu(\text{CO})$ spectra of solutions of $\text{Co}_2(\text{CO})_8$ indicate equilibrium between this dibridged structure and an unbridged structure suggested to have D_{3d} symmetry [34–36]. A third isomer of $\text{Co}_2(\text{CO})_8$, also unbridged, was subsequently suggested from a more detailed study of the solution spectra [37–39].

The computational studies on $\text{Co}_2(\text{CO})_8$ led to optimized structures for both dibridged and unbridged structures (Fig. 3). The relative stabilities of the dibridged and unbridged isomers of $\text{Co}_2(\text{CO})_8$ depend upon the computational method used with the B3LYP and BP86 methods giving opposite orders of isomer stabilities. The Co–Co distance was found to be shorter by ~ 0.11 Å in the dibridged isomer relative to the unbridged isomer indicating a bond-shortening effect of the two bridging carbonyl groups. This phenomenon is generally observed upon comparing bridged and unbridged isomers of binuclear metal carbonyls when the nominal metal–metal bond order remains the same.

Figure 4 shows how the optimized unsaturated binuclear cobalt carbonyl structures [i.e., $\text{Co}_2(\text{CO})_x$, $x = 7, 6, 5$] can be derived from either the dibridged or unbridged structure of $\text{Co}_2(\text{CO})_8$. Thus loss of a carbonyl group from the unbridged isomer of $\text{Co}_2(\text{CO})_8$ leads to the optimized structure for $\text{Co}_2(\text{CO})_7$, whereas losses of terminal carbonyl groups from the dibridged isomer of $\text{Co}_2(\text{CO})_8$ leads to the optimized structures for the more highly unsaturated $\text{Co}_2(\text{CO})_6$ and $\text{Co}_2(\text{CO})_5$.

The 18-electron rule would require a cobalt carbonyl of stoichiometry $\text{Co}_2(\text{CO})_7$ to have a Co=Co double bond. The optimized structure of $\text{Co}_2(\text{CO})_7$ (Fig. 5) has C_{2v} symmetry with no bridging carbonyl groups and with one cobalt bearing four essentially terminal CO groups and the other cobalt bearing only three such CO groups. This structure is closely related to the structure inferred for the isolable, but unstable, $\text{CoRh}(\text{CO})_7$ on the basis of its infrared $\nu(\text{CO})$ frequencies (Fig. 5) [12]. In addition, Sweany and Brown [40] have interpreted the change in the $\nu(\text{CO})$ spectrum upon photolysis of $\text{Co}_2(\text{CO})_8$ in a low-temperature matrix to indicate decarbonylation to $\text{Co}_2(\text{CO})_7$. Table 3 compares the infrared $\nu(\text{CO})$ frequencies calculated for $\text{Co}_2(\text{CO})_7$ with those assigned to $\text{Co}_2(\text{CO})_7$ in the matrix isolation study [40] and with those determined experimentally for $\text{CoRh}(\text{CO})_7$. The correspondence is seen to be very close. The metal–metal bond in C_{2v} - $\text{Co}_2(\text{CO})_7$, as well as that in the analogous $\text{CoRh}(\text{CO})_7$, can be considered to be a single bond with the metal atom bearing four CO groups having the favored 18-electron con-

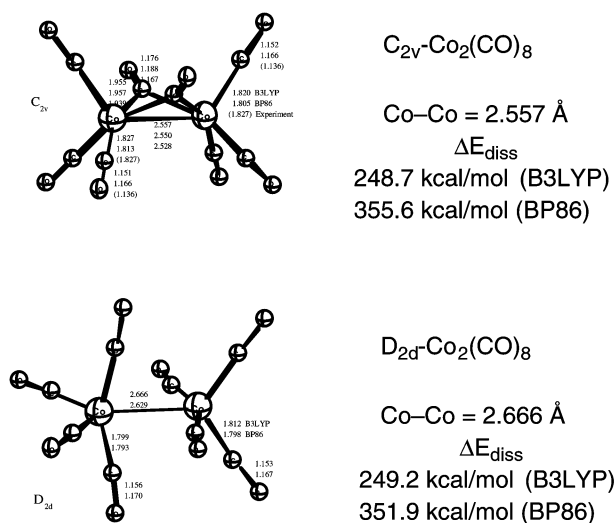


Fig. 3 The optimized dibridged and unbridged structures of $\text{Co}_2(\text{CO})_8$.

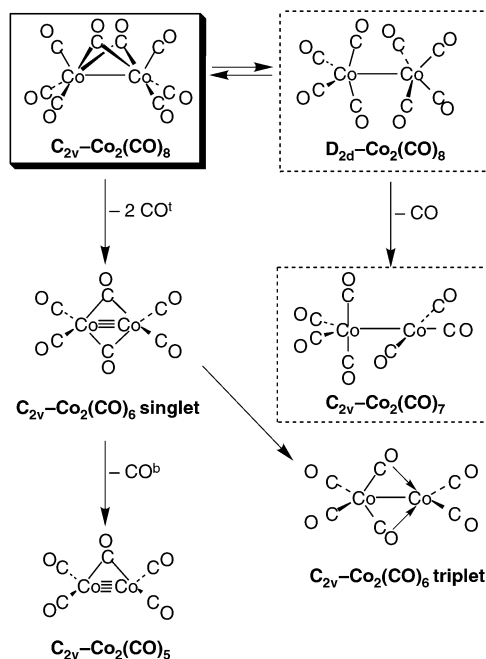


Fig. 4 Generation of the optimized structures for $\text{Co}_2(\text{CO})_x$ ($x = 7, 6, 5$) by the decarbonylation of $\text{Co}_2(\text{CO})_8$. Experimentally measured infrared $\nu(\text{CO})$ frequencies have been assigned to the structures enclosed in dashed boxes.

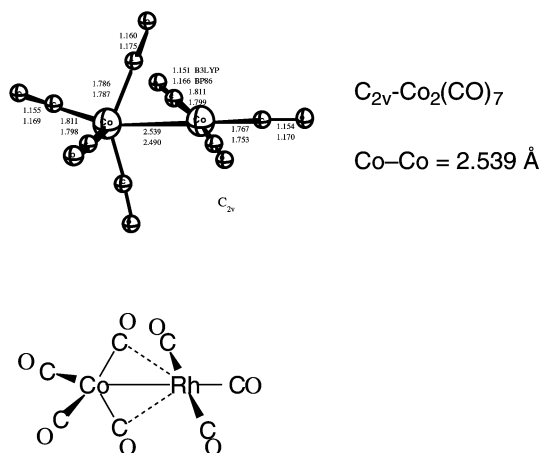


Fig. 5 Comparison of the optimized structure for $\text{Co}_2(\text{CO})_7$ with the structure proposed for the known $\text{CoRh}(\text{CO})_7$ on the basis of its infrared $\nu(\text{CO})$ frequencies.

figuration and the metal atom bearing only three CO groups having a 16-electron configuration similar to square planar d^8 transition-metal complexes. The shorter Co-Co single bond distance (2.54 Å) in $C_{2v}\text{-Co}_2(\text{CO})_7$ (Fig. 5) relative to that in unbridged $\text{Co}_2(\text{CO})_8$ (2.66 Å) can be a consequence of the non-equivalence of the cobalt atoms in $C_{2v}\text{-Co}_2(\text{CO})_7$. This can lead to some ionic character in the Co-Co bond and thus some electrostatic bond-shortening.

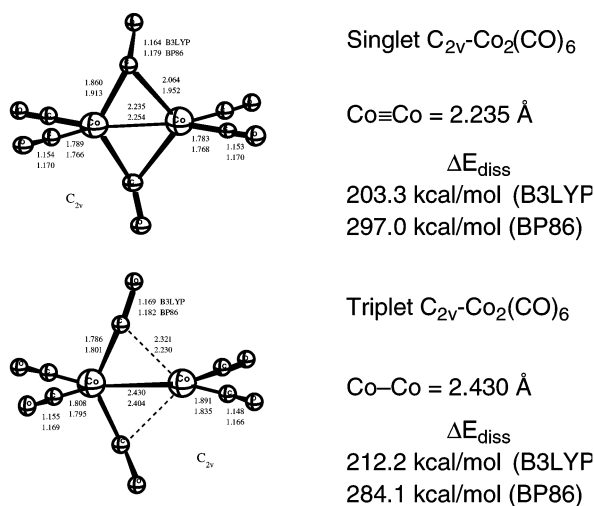
Table 3 Infrared spectra of $\text{Co}_2(\text{CO})_7$ and $\text{CoRh}(\text{CO})_7$.

Compound	$\nu(\text{CO})$ frequencies, cm^{-1}
$\text{Co}_2(\text{CO})_7$ calcd. (BP86)	2080w, 2028m, 2009s, 2009s, 1987w, 1976m, 1958s
$\text{Co}_2(\text{CO})_7$ expt. [40]	2123w, 2066m, 2063m, 2053s, 1967m, 1957m, 1947m
$\text{CoRh}(\text{CO})_7$ expt. [12]	2134w, 2064s, 2058s, 2049vs, 2006m, 1977w, 1955m

Double decarbonylation of $\text{Co}_2(\text{CO})_8$ leads to $\text{Co}_2(\text{CO})_6$, which requires a formal $\text{Co}\equiv\text{Co}$ triple bond for the metal atoms to have the favored 18-electron rare gas electronic configuration. A singlet C_{2v} isomer of $\text{Co}_2(\text{CO})_6$ is found to be an energy minimum with a short cobalt–cobalt bond distance (2.234 Å) suggestive of a $\text{Co}\equiv\text{Co}$ triple bond (Fig. 6). However, there is also a triplet isomer of $\text{Co}_2(\text{CO})_6$, likewise of C_{2v} symmetry, with a very similar energy to that of this singlet C_{2v} - $\text{Co}_2(\text{CO})_6$ isomer. The relative energies of singlet and triplet C_{2v} - $\text{Co}_2(\text{CO})_6$ depend upon the computational method used. Conversion of singlet C_{2v} - $\text{Co}_2(\text{CO})_6$ to its triplet isomer results in lengthening of the cobalt–cobalt bond from 2.234 to 2.430 Å with concurrent conversion of the nearly symmetrical bridging CO groups to highly unsymmetrical bridging CO groups.

The double decarbonylation of $\text{Co}_2(\text{CO})_8$ to give $\text{Co}_2(\text{CO})_6$ with a formal $\text{Co}\equiv\text{Co}$ triple bond suggested by these computational studies (Fig. 4) is analogous to the experimentally observed double decarbonylation of $(\text{C}_5\text{H}_5)_2\text{Mo}_2(\text{CO})_6$ to give $(\text{C}_5\text{H}_5)_2\text{Mo}_2(\text{CO})_4$ with a likewise formal $\text{Mo}\equiv\text{Mo}$ triple bond (Fig. 7). However, the decrease in the metal–metal bond distance in going from $(\text{C}_5\text{H}_5)_2\text{Mo}_2(\text{CO})_6$ to $(\text{C}_5\text{H}_5)_2\text{Mo}_2(\text{CO})_4$ (~ 0.8 Å) is much larger than that in going from $\text{Co}_2(\text{CO})_8$ to $\text{Co}_2(\text{CO})_6$ (0.32 Å). This probably relates to an unusually long Mo–Mo single bond distance in $(\text{C}_5\text{H}_5)_2\text{Mo}_2(\text{CO})_6$ [41] owing to the lack of bridging CO groups and the steric repulsion between the C_5H_5 rings and terminal CO groups on each metal atom.

Continuing the decarbonylation of $\text{Co}_2(\text{CO})_8$ (Fig. 4) leads to the triple decarbonylation product $\text{Co}_2(\text{CO})_5$ required to have a formal $\text{Co}\equiv\text{Co}$ quadruple bond for the metal atoms each to have the favored 18-electron configuration. An energy minimum with no significant imaginary vibrational frequencies is actually found by both computational methods (B3LYP and BP86) for $\text{Co}_2(\text{CO})_5$. This

**Fig. 6** The optimized singlet and triplet structures for $\text{Co}_2(\text{CO})_6$.

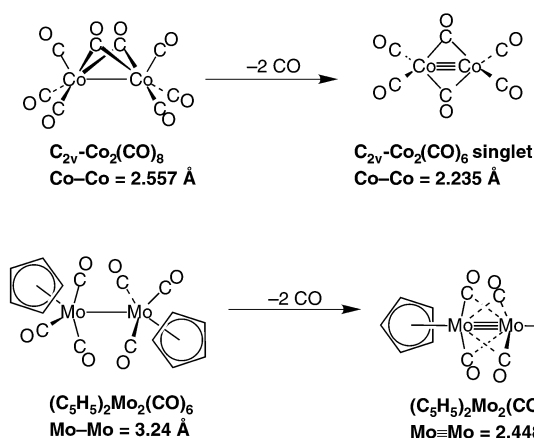


Fig. 7 Comparison of the double decarbonylations of $\text{Co}_2(\text{CO})_8$ and $(\text{C}_5\text{H}_5)_2\text{Mo}_2(\text{CO})_6$ to give the corresponding species with metal–metal triple bonds.

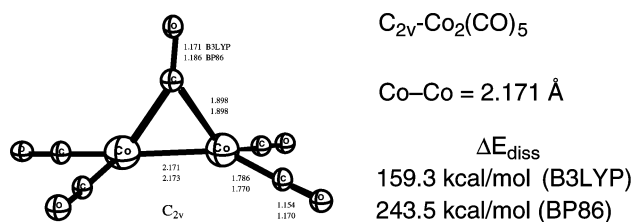


Fig. 8 The optimized structure of $\text{Co}_2(\text{CO})_5$, postulated to have a $\text{Co}\equiv\text{Co}$ quadruple bond.

structure (Fig. 8) has a single bridging carbonyl group and a cobalt–cobalt distance (2.171 Å) even shorter than that assigned to the triple bond in $\text{Co}_2(\text{CO})_6$ suggestive of a possible $\text{Co}\equiv\text{Co}$ quadruple bond. Triplet isomers of $\text{Co}_2(\text{CO})_5$ were computed to have high imaginary vibrational frequencies ($>100i \text{ cm}^{-1}$) suggesting that they are saddle points rather than true minima. No examples of binuclear metal carbonyl derivatives having formal metal–metal quadruple bonds have been found experimentally, even in the case of cyclopentadienylmetal carbonyls, where a variety of unsaturated metal–metal multiply bonded derivatives have been isolated and characterized structurally [6].

Attempts to decarbonylate $\text{Co}_2(\text{CO})_8$ by heating to give the $\text{Co}_2(\text{CO})_x$ ($x = 7, 6, 5$) isomers depicted in Fig. 4 have all failed because of the facile conversion of $\text{Co}_2(\text{CO})_8$ to $\text{Co}_4(\text{CO})_{12}$ only slightly above room temperature [5,42]. Kinetics of this conversion of $\text{Co}_2(\text{CO})_8$ to $\text{Co}_4(\text{CO})_{12}$ suggest the following rate law [43,44] where $n = 2$ (hexane) to 4 (toluene):

$$\text{rate} = \frac{d[\text{Co}_4(\text{CO})_{12}]}{dt} = k_{\text{obs}} \frac{[\text{Co}_2(\text{CO})_8]^2}{[\text{CO}]^n} \quad (3)$$

This rate law has been interpreted to suggest the following mechanism for conversion of $\text{Co}_2(\text{CO})_8$ into $\text{Co}_4(\text{CO})_{12}$:





These observations suggest that $\text{Co}_2(\text{CO})_6$ is unstable with respect to dimerization leading ultimately to a tetrahedrane derivative, possibly through a cyclobutadiene-type intermediate (Fig. 9) similar to the dimerization of certain acetylenes.

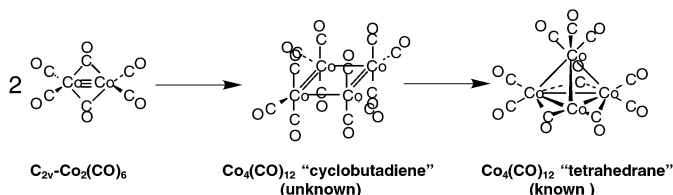


Fig. 9 Dimerization of $\text{Co}_2(\text{CO})_6$ to the known "tetrahedrane" $\text{Co}_4(\text{CO})_{12}$ through a "cyclobutadiene" $\text{Co}_4(\text{CO})_{12}$ intermediate.

Iron carbonyls

Figure 10 shows the decarbonylation of $\text{Fe}_2(\text{CO})_9$ to give unsaturated binuclear iron carbonyl derivatives $\text{Fe}_2(\text{CO})_x$ ($x = 8, 7,$ and 6) found to be minima in the computations. The lowest energy isomer for the single decarbonylation product $\text{Fe}_2(\text{CO})_8$ is the C_{2v} dibridged isomer formed by loss of one of the bridging CO groups from $\text{Fe}_2(\text{CO})_9$ (Fig. 11). The 2.52 \AA Fe–Fe distance in $\text{Fe}_2(\text{CO})_9$ decreases to 2.44 \AA in dibridged $\text{C}_{2v}\text{-Fe}_2(\text{CO})_8$ in accord with the increase in the formal bond order from one to two in order to maintain the favored 18-electron configuration about each iron atom. An unbridged C_{2h} isomer of $\text{Fe}_2(\text{CO})_8$ has also been found as a local minimum at 2.0 (B3LYP) to 4.2 (BP86) kcal/mol higher in energy than C_{2v} dibridged $\text{Fe}_2(\text{CO})_8$ (Fig. 11). The Fe=Fe distance (2.61 \AA) in the C_{2h} unbridged $\text{Fe}_2(\text{CO})_8$ is 0.16 \AA longer than the Fe=Fe distance in dibridged $\text{C}_{2v}\text{-Fe}_2(\text{CO})_8$ despite the same formal iron–iron bond order. This is another example of metal–metal bond-shortening by bridging CO groups.

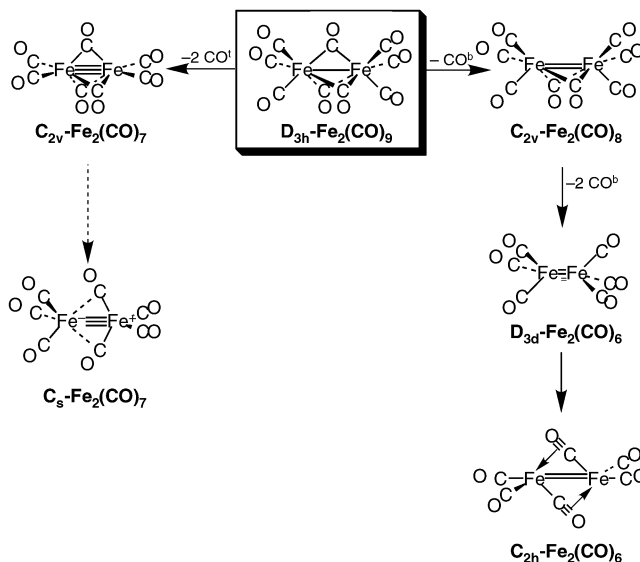


Fig. 10 Generation of the optimized structures for $\text{Fe}_2(\text{CO})_x$ ($x = 8, 7, 6$) by the decarbonylation of $\text{Fe}_2(\text{CO})_9$.

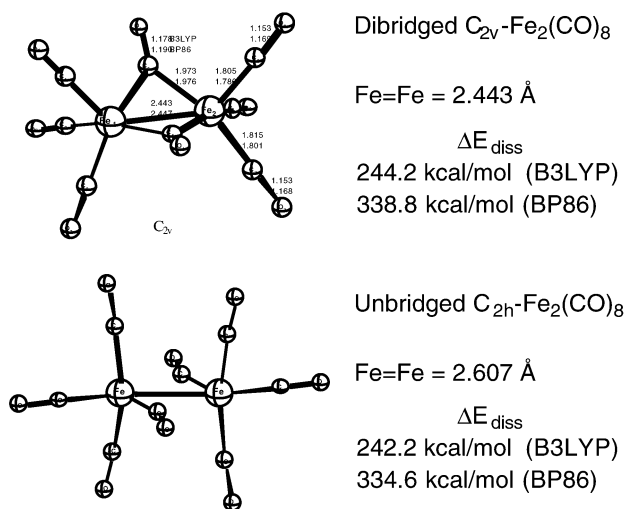


Fig. 11 The optimized dibridged and unbridged structures of $Fe_2(CO)_8$.

Matrix isolation studies by Fletcher, Poliakoff, and Turner [45] provide experimental evidence for dibridged C_{2v} - $Fe_2(CO)_8$. Thus, photolysis of $Fe_2(CO)_9$ in argon matrices at 15 K was found to give a $\nu(\text{CO})$ spectrum interpreted to be the dibridged C_{2v} - $Fe_2(CO)_8$. The experimental $\nu(\text{CO})$ infrared spectrum for dibridged C_{2v} - $Fe_2(CO)_8$ is close to that calculated in our work (Table 4). Experimental evidence was also obtained for an unbridged isomer of $Fe_2(CO)_8$. Table 4 compares the calculated $\nu(\text{CO})$ frequencies for the lowest energy unbridged isomer of $Fe_2(CO)_8$ with the experimental $\nu(\text{CO})$ frequencies assigned to unbridged $Fe_2(CO)_8$. The general patterns of the experimental and calculated frequencies for unbridged $Fe_2(CO)_8$ are similar, although the agreement is not as close as that for the dibridged C_{2v} - $Fe_2(CO)_8$. However, the $\nu(\text{CO})$ frequencies for unbridged $Fe_2(CO)_8$ were considerably more difficult to obtain than those for dibridged C_{2v} - $Fe_2(CO)_8$ because of the smaller concentrations of the unbridged isomer in the low-temperature photolysis mixtures.

Loss of two terminal carbonyl groups from $Fe_2(CO)_9$ gives a tribridged C_{2v} isomer $Fe_2(CO)_7$ as an optimized structure with a computed $Fe\equiv Fe$ distance of 2.212 Å. This distance is ~ 0.3 Å shorter than the $Fe-Fe$ distance in $Fe_2(CO)_9$, in accord with an increase in the formal iron–iron bond order from one to three corresponding to retention of 18-electron configurations around each iron atom (Fig. 12). However, of still lower energy by 9.9 (B3LYP) to 13.7 (BP86) kcal/mol is a less symmetrical C_s structure with two semibridging CO groups. The iron–iron distance changes relatively little (~ 0.02 Å) in going from C_{2v} - $Fe_2(CO)_7$ to C_s - $Fe_2(CO)_7$ (Fig. 12). The C_s structure of $Fe_2(CO)_7$ is closely related to the structure determined by X-ray diffraction [46,47] for the known [48] $(C_5H_5)_2V_2(CO)_5$ by substitution of one terminal CO group on each iron atom by a pentahapto cyclopentadienyl ring with the nec-

Table 4 Infrared spectra of $Fe_2(CO)_8$ isomers.

Compound	$\nu(\text{CO})$ frequencies, cm^{-1}
C_{2v} - $Fe_2(CO)_8$ calcd. (BP86)	2030s, 2006s, 2001s, 1870w, 1841m
Bridged isomer of $Fe_2(CO)_8$, expt. [45]	2055s, 2032s, 2022s, 1857w, 1814m
C_{2h} - $Fe_2(CO)_8$ calcd. (BP86)	2015s, 1998s, 1985m, 1901m
Unbridged isomer of $Fe_2(CO)_8$, expt. [45]	2038s, 2006s, 1978w, 1974w

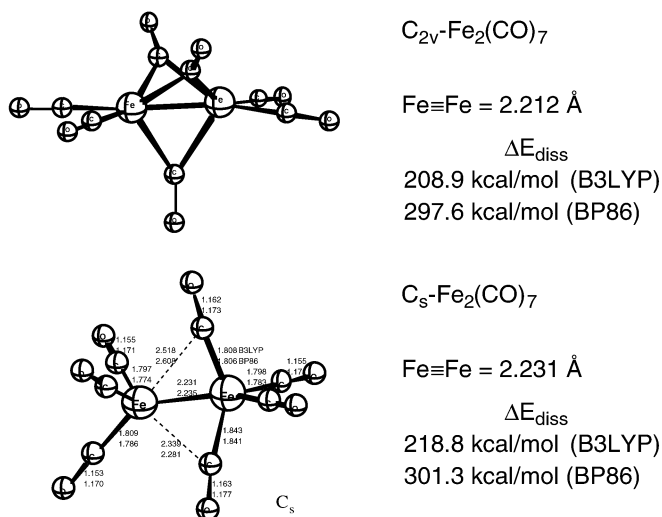


Fig. 12 The optimized C_{2v} and C_s isomers of $\text{Fe}_2(\text{CO})_7$.

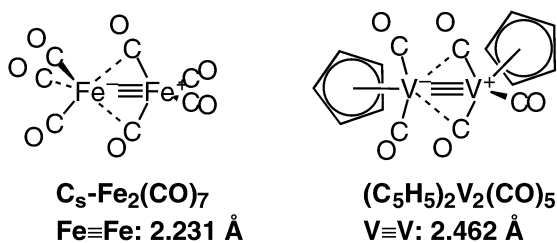


Fig. 13 Analogy between the optimized $C_s\text{-Fe}_2(\text{CO})_7$ structure and the known $(\text{C}_5\text{H}_5)_2\text{V}_2(\text{CO})_5$ structure, including their formation from $\text{Fe}(\text{CO})_5$ and $(\eta^5\text{-C}_5\text{H}_5)\text{V}(\text{CO})_4$, respectively.

essary adjustment of the central metal atom from iron to vanadium to retain the same metal electronic configuration (Fig. 13). Both compounds are derived from stable mononuclear metal carbonyls [$\text{Fe}(\text{CO})_5$ and $\text{C}_5\text{H}_5\text{V}(\text{CO})_4$, respectively] by loss of 1.5 CO groups per metal atom. In addition, both compounds have relatively short metal–metal bond distances suggestive of metal–metal multiple bonding, probably of order three.

Computational studies have also been done on $\text{Fe}_2(\text{CO})_6$, which would be expected to have a formal $\text{Fe}\equiv\text{Fe}$ quadruple bond if both iron atoms have the favored 18-electron configuration. An optimized structure with imaginary frequencies $<20i \text{ cm}^{-1}$ was found for an unbridged D_{3d} isomer of $\text{Fe}_2(\text{CO})_6$ formed by loss of the three bridging CO groups from $\text{Fe}_2(\text{CO})_9$. The iron–iron distance decreases from 2.52 Å in $\text{Fe}_2(\text{CO})_9$ to only 2.00 Å in this $\text{Fe}_2(\text{CO})_6$ structure consistent with an increase in the metal–metal bond order from one to four (Fig. 14). However, a less symmetrical C_{2h} isomer of $\text{Fe}_2(\text{CO})_6$ with two unsymmetrical bridging CO groups was found to be 13.2 (B3LYP) to 16.4 (BP86) kcal/mol lower in energy than unbridged $D_{3d}\text{-Fe}_2(\text{CO})_6$. The iron–iron distance increases from 2.00 Å in unbridged $D_{3d}\text{-Fe}_2(\text{CO})_6$ to 2.44 Å in unsymmetrically dibridged $C_{2h}\text{-Fe}_2(\text{CO})_6$ consistent with a decrease in the formal iron–iron bond order from four to two. An unsymmetrically dibridged

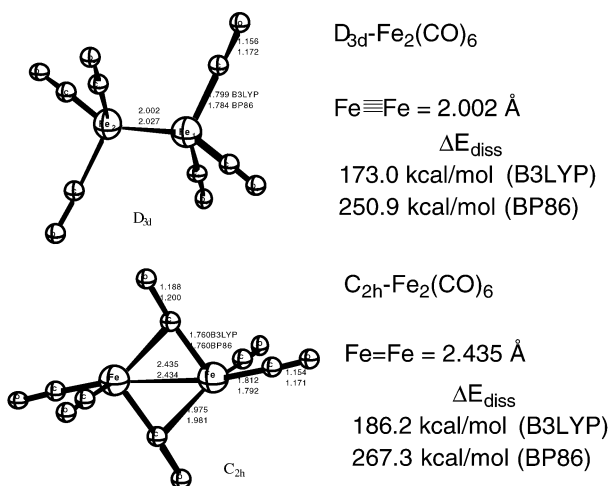


Fig. 14 The optimized structures for $\text{Fe}_2(\text{CO})_6$.

$C_{2h}\text{-Fe}_2(\text{CO})_6$ with a formal $\text{Fe}=\text{Fe}$ bond order of two can retain the favored 18-electron configurations for the iron atoms if the unsymmetrically bridging CO groups are four-electron donors rather than the usual two-electron donors because of π -donation from the carbon–oxygen multiple bond.

SUMMARY

Computational methods, which have been shown to give computed geometrical parameters and energies closed to experimental values for known metal carbonyls such as $\text{Fe}(\text{CO})_5$, $\text{Fe}_2(\text{CO})_9$, and $\text{Fe}_3(\text{CO})_{12}$, have been extended to unsaturated binary binuclear metal carbonyls. Optimized structures have been found exhibiting the following features: (a) metal–metal multiple bonds with the favored 18-electron rare gas metal electronic configuration such as the formal $\text{M}=\text{M}$ double bonds in $\text{Ni}_2(\text{CO})_6$ and $\text{Fe}_2(\text{CO})_8$ and the formal $\text{M}\equiv\text{M}$ triple bonds in $\text{Ni}_2(\text{CO})_5$, $\text{Co}_2(\text{CO})_6$, and $\text{Fe}_2(\text{CO})_7$; (b) four-electron bridging carbonyl groups with the favored 18-electron metal electronic configuration such as in C_{2h} symmetry $\text{Fe}_2(\text{CO})_6$; (c) metal electronic configurations with less than 18 electrons, such as the 16-electron configurations for d^8 metal atoms found in the unbridged $\text{Co}_2(\text{CO})_7$ analogous to the known $\text{CoRh}(\text{CO})_7$. Some analogies have been observed between optimized computed structures for unsaturated binary metal carbonyls and known structurally characterized cyclopentadienylmetal carbonyls such as the formal metal–metal triple bonds in C_{2v} symmetry $\text{Co}_2(\text{CO})_6$ and $(\text{C}_5\text{H}_5)_2\text{Mo}_2(\text{CO})_4$ and the metal–metal multiple bonds and unsymmetrical bridging carbonyl groups in C_s symmetry $\text{Fe}_2(\text{CO})_7$ and $(\text{C}_5\text{H}_5)_2\text{V}_2(\text{CO})_5$. Computational evidence for formal metal–metal quadruple bonds in metal carbonyls has been found in optimized structures for $\text{Co}_2(\text{CO})_5$ and $\text{Fe}_2(\text{CO})_6$ exhibiting unusually short metal–metal distances.

ACKNOWLEDGMENTS

We thank Dr. Yaoming Xie, Mr. Joseph P. Kenny, and Dr. Igor S. Ignatyev for their contributions to the research described in this Account. This research was supported by the Chemistry Division of the U.S. National Science Foundation.

REFERENCES

1. L. Mond, C. Langer, F. Quincke. *J. Chem. Soc.* **57**, 749 (1890).
2. M. Berthelot. *Compt. Rend. Acad. Sci. Paris* **112**, 1343 (1891).
3. L. Mond and F. Quincke. *J. Chem. Soc.* 604 (1891).
4. J. Dewar and H. O. Jones. *Proc. Roy. Soc. (London)* **A76**, 558 (1905).
5. L. Mond, H. Hirtz, M. D. Cowap. *J. Chem. Soc.* 798 (1910).
6. M. J. Winter. *Adv. Organometal. Chem.* **29**, 101 (1989).
7. R. B. King and M. B. Bisnette. *J. Organomet. Chem.* **7**, 311 (1967).
8. R. J. Klingler, W. Butler, M. D. Curtis. *J. Am. Chem. Soc.* **97**, 3535 (1975); **100**, 5034 (1978).
9. J. S. Huang and L. F. Dahl. *J. Organomet. Chem.* **243**, 57 (1983).
10. R. Colton and C. J. Commons. *Aust. J. Chem.* **28**, 1673 (1975).
11. C. J. Commons and B. F. Hoskins. *Aust. J. Chem.* **28**, 1663 (1975).
12. I. T. Horváth, G. Bor, M. Garland, P. Pino. *Organometallics* **5**, 1441 (1986).
13. J. H. Jang, J. G. Lee, H. Lee, Y. Xie, H. F. Schaefer III. *J. Phys. Chem. A* **102**, 5298 (1998).
14. Ni: I. S. Ignatyev, H. F. Schaefer III, R. B. King, S. T. Brown. *J. Am. Chem. Soc.* **122**, 1989 (2000).
15. Co: J. P. Kenny, R. B. King, H. F. Schaefer III. *Inorg. Chem.* **40**, 900 (2001).
16. Fe: Y. Xie, H. F. Schaefer III, R. B. King. *J. Am. Chem. Soc.* **122**, 8746 (2000).
17. T. H. Dunning. *J. Chem. Phys.* **53**, 2823 (1970).
18. S. Huzinaga. *J. Chem. Phys.* **42**, 1293 (1965).
19. A. J. H. Wachters. *J. Chem. Phys.* **52**, 1033 (1970).
20. D. M. Hood, R. M. Pitzer, H. F. Schaefer III. *J. Chem. Phys.* **71**, 705 (1979).
21. A. D. Becke. *J. Chem. Phys.* **98**, 5648 (1988).
22. C. Lee, W. Yang, R. G. Parr. *Phys. Rev. B* **37**, 785 (1988).
23. A. D. Becke. *Phys. Rev. A* **38**, 3098 (1988).
24. J. P. Perdew. *Phys. Rev. B* **33**, 8822 (1986).
25. M. J. Frisch, G. W. Trucks, H. B. Schlegel, P. M. W. Gill, B. G. Johnson, M. A. Robb, J. R. Cheeseman, T. Keith, G. A. Petersson, J. A. Montgomery, K. Raghavachari, M. A. Al-Laham, V. G. Zakrzewski, J. V. Ortiz, J. B. Foresman, C. Y. Peng, P. Y. Ayala, W. Chen, M. W. Wong, J. L. Andes, E. S. Replogle, R. Gomperts, R. L. Martin, D. J. Fox, J. S. Binkley, D. J. Defrees, J. Baker, J. J. P. Stewart, M. Head-Gordon, C. Gonzalez, J. A. Pople. *Gaussian 94, Revision B.3*, Gaussian Inc., Pittsburgh, PA (1995).
26. E. Speyer and H. Wolf. *Chem. Ber.* **60**, 1924 (1927).
27. F. A. Cotton and J. M. Troup. *J. Am. Chem. Soc.* **96**, 3438 (1974).
28. R. A. Sinclair and A. B. Burg. *Inorg. Chem.* **7**, 2160 (1968).
29. Z.-Z. Zhang, H.-K. Wang, H.-G. Wang, R.-J. Wang, W.-J. Zhao, L.-M. Yang. *J. Organomet. Chem.* **347**, 269 (1988).
30. N. Mézailles, P. Le Floch, K. Waschbüsch, L. Ricard, F. Mathey, C. P. Kubiak. *J. Organomet. Chem.* **541**, 277 (1997).
31. G. G. Sumner, H. P. Klug, L. E. Alexander. *Acta Crystallogr.* **17**, 732 (1964).
32. P. C. Leung and P. Coppens. *Acta Crystallogr.* **B39**, 535 (1983).
33. D. Braga, F. Grepioni, P. Sabatino, A. Gavezzotti. *J. Chem. Soc., Dalton Trans.* 1185 (1992).
34. K. Noack. *Spectrochem. Acta* **19**, 1925 (1963).
35. K. Noack. *Helv. Chim. Acta* **47**, 1065, 1554 (1964).
36. G. Bor. *Spectrochim. Acta* **14**, 1209, 2065 (1963).
37. G. Bor and K. Noack. *J. Organometal. Chem.* **64**, 367 (1974).
38. G. Bor, U. K. Dietler, K. Noack. *Chem. Commun.* 914 (1976).
39. S. Onaka and D. F. Shriver. *Inorg. Chem.* **15**, 915 (1976).
40. R. L. Sweany and T. L. Brown. *Inorg. Chem.* **16**, 421 (1977).

41. R. D. Adams, D. M. Collins, F. A. Cotton. *Inorg. Chem.* **13**, 1086 (1974).
42. R. Ercoli, P. Chini, M. Massimauri. *Chim. e Ind. (Milan)* **41**, 132 (1959).
43. F. Ungváry and L. Markó. *Inorg. Chim. Acta* **4**, 324 (1970).
44. F. Ungváry and L. Markó. *J. Organomet. Chem.* **71**, 283 (1974).
45. S. C. Fletcher, M. Poliakoff, J. J. Turner. *Inorg. Chem.* **25**, 3597 (1986).
46. F. A. Cotton, L. Kurczynski, B. A. Frenz. *J. Organomet. Chem.* **160**, 93 (1978).
47. J. C. Huffman, L. N. Lewis, K. G. Caulton. *Inorg. Chem.* **19**, 2785 (1980).
48. E. O. Fischer and R. J. Schneider. *Chem. Ber.* **103**, 3684 (1970).